Copyright © 1991, by the author(s).
All rights reserved.

Permission to make digital or hard copies of all or part of this work for personal or classroom use is granted without fee provided that copies are not made or distributed for profit or commercial advantage and that copies bear this notice and the full citation on the first page. To copy otherwise, to republish, to post on servers or to redistribute to lists, requires prior specific permission.

EXPERIMENTAL CHAOS VIA CHUA'S CIRCUIT

by

Michael Peter Kennedy

Memorandum No. UCB/ERL M91/95

28 October 1991

EXPERIMENTAL CHAOS VIA CHUA'S CIRCUIT

by

Michael Peter Kennedy

Memorandum No. UCB/ERL M91/95

28 October 1991

ELECTRONICS RESEARCH LABORATORY

College of Engineering
University of California, Berkeley
94720

TITLE PAGE

EXPERIMENTAL CHAOS VIA CHUA'S CIRCUIT

by

Michael Peter Kennedy

Memorandum No. UCB/ERL M91/95

28 October 1991

ELECTRONICS RESEARCH LABORATORY

College of Engineering
University of California, Berkeley
94720

EXPERIMENTAL CHAOS VIA CHUA'S CIRCUIT

Michael Peter Kennedy
Electronics Research Laboratory
University of California, Berkeley, CA 94720

Abstract

Chua's circuit is a simple electronic network which exhibits a variety of bifurcation phenomena and attractors. The circuit consists of two capacitors, an inductor, a linear resistor, and a nonlinear resistor. This paper presents a simple and robust practical implementation of Chua's circuit.

1 Introduction

Chua's circuit [Mat84], shown in Fig. 1, is a simple oscillator circuit which exhibits a variety of bifurcations and chaos. The circuit contains three linear energy-storage elements (an inductor and two capacitors), a linear resistor, and a single nonlinear resistor N_R. The nonlinear resistor has a three-segment piecewise-linear driving point characteristic, as shown in Fig. 2.

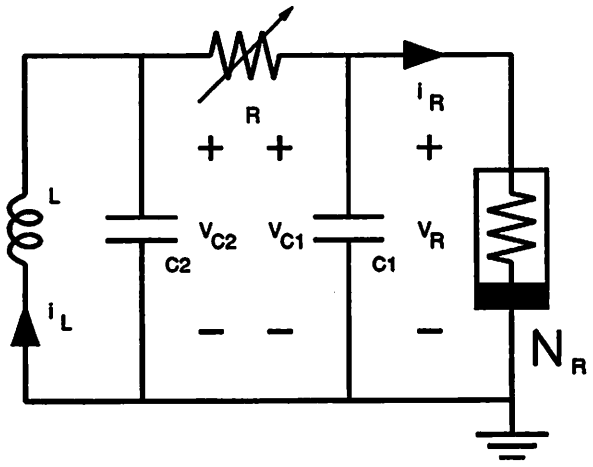

Figure 1: Chua's circuit consists of a linear inductor L, a linear resistor R, two linear capacitors C_1 and C_2, and a nonlinear resistor N_R.

In the first reported study of this circuit, Matsumoto [Mat84] showed by computer simulation that the system possesses a strange attractor called the Double Scroll. Experimental confirmation of

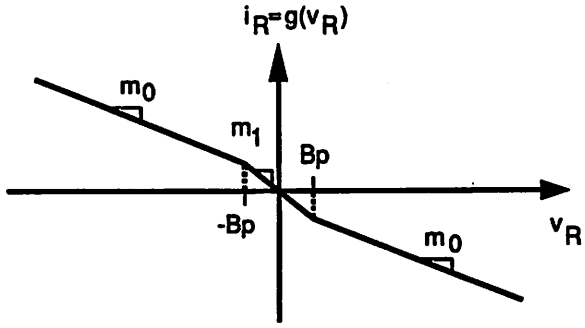

Figure 2: Three-segment piecewise-linear $v - i$ characteristic of the nonlinear resistor in Chua's circuit. The outer regions have slopes m_0; the inner region has slope m_1. There are two breakpoints at $\pm B_P$.

the presence of this attractor was made shortly afterwards by Zhong and Ayrom [ZA85a]. Since then, the system has been studied extensively; a variety of bifurcation phenomena and chaotic attractors in the circuit have been discovered experimentally and confirmed mathematically [CKM86, KC87, MC87, Kah88a, Kah88b, Kah88c, Kom88a, Kom88b, MCA88, Kom90, Kah91, KTMH91, LU91].

Most of the experimental studies of Chua's circuit have appeared in the Electronics Engineering literature [MCK85, CKM86, MCK86, Bro87, MCK87, Ogo87, YL87, BT90]. This paper is directed at a broader audience of experimentalists who have not thus far considered studying bifurcation phenomena in electronic circuits.

While mechanical systems provide a convenient framework in which to examine bifurcations and chaos, electronic circuits are unique in being easy to build, easy to measure, and easy to model. In particular, Chua's circuit and its relatives [CKM86, MCT87, PC87, Wu87, BC88, SC88, CL90a], which are readily constructed and modeled, can exhibit every type of bifurcation and attractor which has been reported to date in third-order continuous-time dynamical systems [ZA85b, TMIM89, TMK+89, CL90b]. In this paper, we provide a simple implementation of Chua's circuit with the aim of encouraging experimentalists to select electronic circuits rather than mass-spring-damper systems as the metaphor of choice for studying the physical world.

2 Practical realization of Chua's Circuit

Chua's circuit can be realized in a variety of ways using standard or custom-made electronic components. Since the linear elements (the capacitor, resistor, and inductor) are readily available as two-terminal devices, our principal concern here is with circuitry to realize the nonlinear resistor.

Several implementations of this element already exist in the literature; these use operational amplifiers [ZA85a], diodes [Mat84], transistors [MCT86], and operational transconductance amplifiers [CC91].

The circuit which we present in the following sections is for demonstration, research, and educational purposes. While it may appear more complicated than earlier implementations in that the nonlinear resistor comprises two operational amplifiers (op amps), it is possible to buy two op amps in a single package. Thus, our circuit uses a minimum number of components: a pair of op amps and six resistors to implement the negative resistor, two capacitors, an inductor, and a variable resistor.

2.1 Realization of nonlinear resistor for Chua's circuit using two op amps and six resistors

Our objective is to construct a two-terminal resistive element with the three-segment piecewise-linear $v - i$ characteristic shown in Fig. 2. This can be done with the subcircuit labelled N_R in Fig. 3. The nonlinear resistor is formed by the two op amps A_1 and A_2 (powered by two 9V batteries), and six linear resistors R_1–R_6.

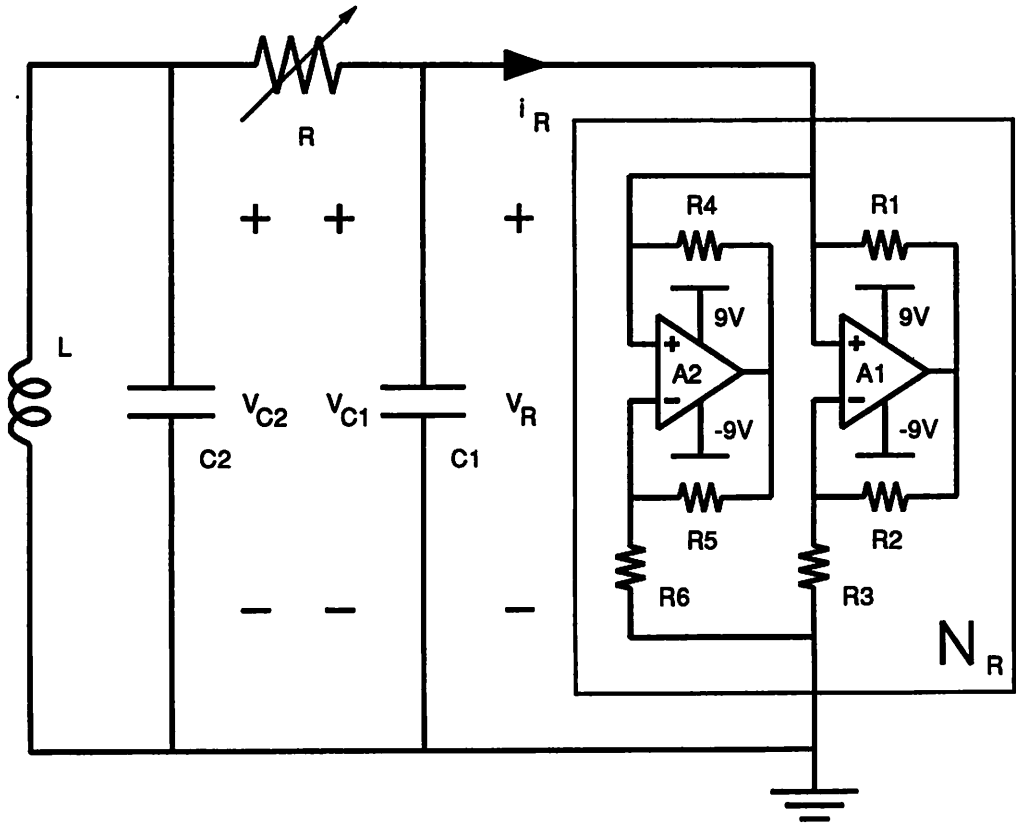

Figure 3: Realization of Chua's circuit using two op amps and six linear resistors to implement N_R. The two op amps are available in a single eight-pin package.

The important feature of the $v - i$ characteristic is that it possesses three regions of negative slope. The breakpoints between the linear regions are proportional to the saturation levels of the op amps. Each op amp provides one pair of breakpoints, so the entire $v - i$ characteristic actually consists of five segments, rather than three, as shown in Fig. 4. As long as the voltages and currents on the attractor are restricted to the negative resistance region of the characteristic, these outer segments will not affect the circuit's behavior.

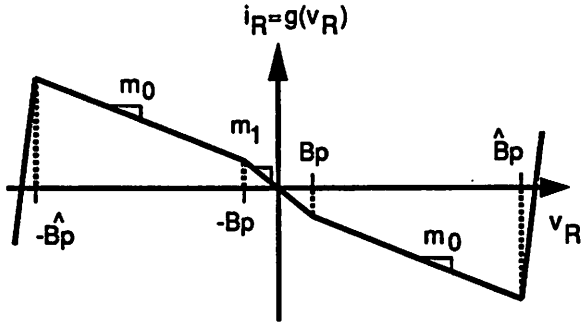

Figure 4: Op amp realization consists of five piecewise-linear segments. If the dynamics are confined to the regions of negative slope, we need not consider the outer segments.

2.1.1 Practical implementation of Chua's circuit

Fig. 5 shows a practical implementation of Chua's circuit using an Analog Devices AD712 dual BiFET op amp, two 9V batteries, and six resistors to implement the negative resistor.

A complete component list for this circuit is given below. In addition to the components listed, we recommend that a bypass capacitor C of at least $0.1\mu F$ be connected across each power supply, as shown in Fig. 5, as close to the op amp as possible. The purpose of these capacitors is to maintain the power supplies at a steady dc voltage.

2.1.2 Component list

Element	Description	Value	Tolerance
A_1	Op amp ($\frac{1}{2}$ AD712, TL082, or equivalent)		
R_1	$\frac{1}{4}$W Resistor	220 Ω	±5%
R_2	$\frac{1}{4}$W Resistor	220 Ω	±5%
R_3	$\frac{1}{4}$W Resistor	2.2 kΩ	±5%
A_2	Op amp ($\frac{1}{2}$ AD712, TL082, or equivalent)		
R_4	$\frac{1}{4}$W Resistor	22 kΩ	±5%
R_5	$\frac{1}{4}$W Resistor	22 kΩ	±5%
R_6	$\frac{1}{4}$W Resistor	3.3 kΩ	±5%
C_1	Capacitor	10 nF	±5%
R	Potentiometer	2 kΩ	
C_2	Capacitor	100 nF	±5%
L	Inductor (TOKO type 10RB or equivalent)	18 mH	± 10%

The slopes of the resulting nonlinear $v - i$ characteristic are given by $m_0 = -\frac{R_2}{R_1 R_3} + \frac{1}{R_4} = -0.409mA/V$, and $m_1 = -\frac{R_2}{R_1 R_3} - \frac{R_5}{R_4 R_6} = -0.758mA/V$. The breakpoints are determined by the saturation voltages E_{sat} of the op amps: $\hat{B}_P = \frac{R_3}{R_2+R_3} E_{sat} \approx 7.61V$ and $B_P = \frac{R_6}{R_5+R_6} E_{sat} \approx 1.08V$, when $E_{sat} \approx 8.3V$.

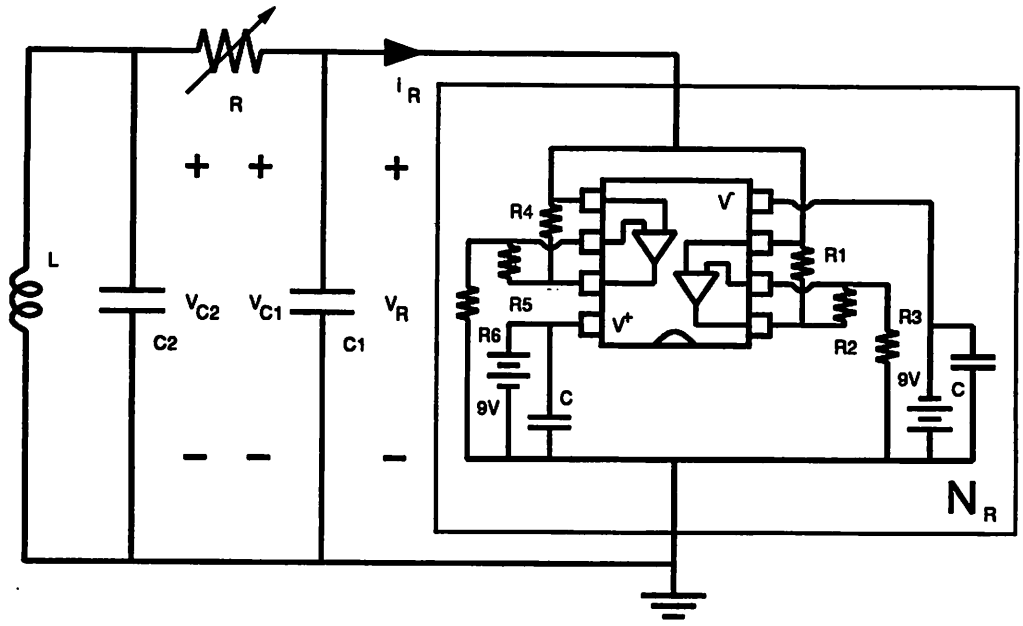

Figure 5: Practical realization of Chua's circuit using an eight-pin dual op amp integrated circuit.

2.1.3 Experimental verification of $v - i$ characteristic

The $v - i$ characteristic of the nonlinear resistor N_R can be measured in isolation by means of the circuit shown in Fig 6.

Resistor R_S, known as a current-sensing resistor, is used to measure the current i_R which flows into the negative resistor N_R when a voltage v_R is applied across its terminals. An appropriate choice of R_S in this example is 100 Ω. Current i_R flowing in R_S then causes a voltage $v_{i_R} = -100 i_R$ to appear across the sensing resistor. Thus, we can measure the $v - i$ characteristic of N_R by applying a voltage v_S as shown and plotting $v_{i_R} (\propto -i_R)$ versus v_R. This is achieved by connecting v_{i_R} to the Y-input and v_R to the X-input of an oscilloscope in X-Y mode. The resulting characteristic for the components listed in the table is shown in Fig 7. Note that we have plotted $-v_{i_R}$ versus v_R; this is possible if your oscilloscope permits inversion of the Y-input in X-Y mode.

3 Bifurcations and Chaos

3.1 R bifurcation sequence

By reducing the variable resistor R from 2000 Ω towards zero, Chua's circuit exhibits a sequence of bifurcations from dc equilibrium through a Hopf bifurcation and period-doubling sequence to a Rössler-type attractor and the Double Scroll strange attractor, as illustrated in Fig. 8. A two-dimensional projection of the attractor is obtained by connecting v_{C_1} and v_{C_2} to the X and Y channels, respectively, of an X-Y oscilloscope.

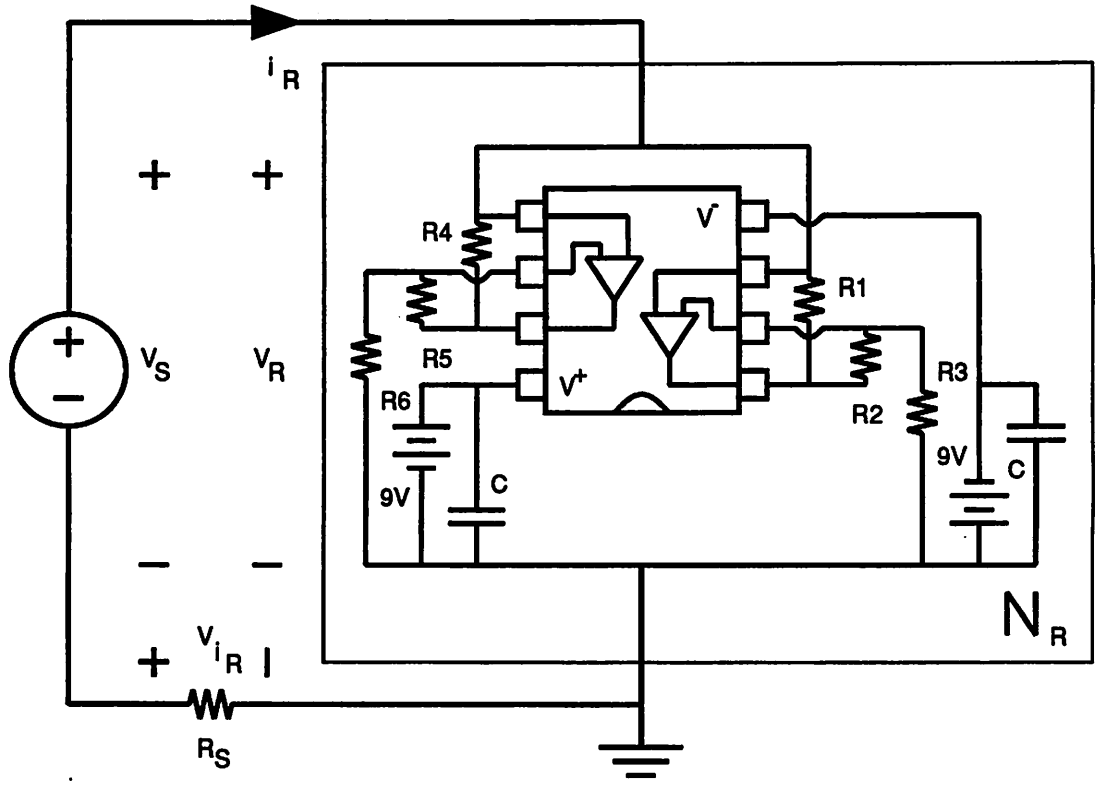

Figure 6: The $v - i$ characteristic of negative resistor N_R can be measured by applying a triangular voltage waveform v_S to the series combination of N_R and a small current-sensing resistor R_S. Plot $-v_{i_R}(\propto i_R)$ versus v_R. The eight-pin dual op amp package is shown from above in schematic form. The reference end of the package is indicated by a dot or a semicircle (shown here).

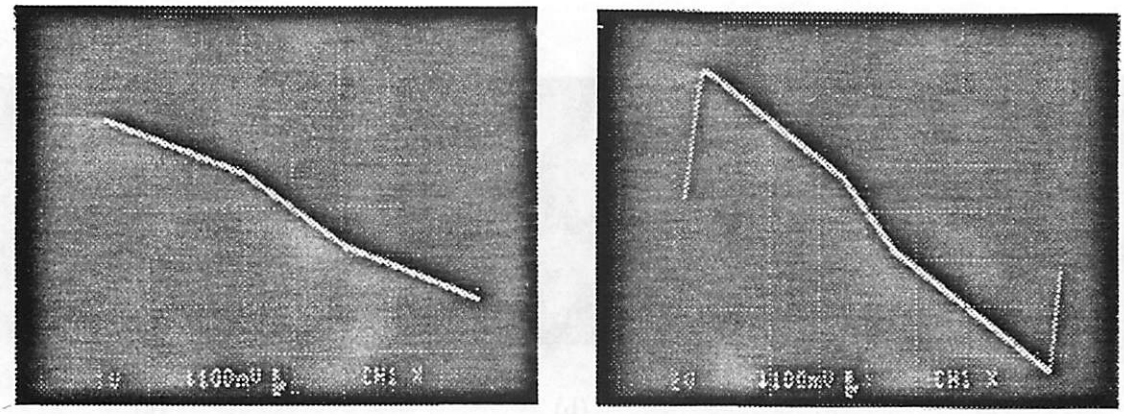

(a) (b)

Figure 7: Measured $v-i$ characteristic of negative resistor. (a) v_S is a triangular waveform with zero dc offset, amplitude 7V peak-to-peak, and frequency 30 Hz. Horizontal axis: v_R (1V/div); Vertical axis: $-v_{i_R}$ (100mV/div); (b) v_S is a triangular waveform with zero dc offset, amplitude 15V peak-to-peak, and frequency 30 Hz. Horizontal axis: v_R (2V/div); Vertical axis: $-v_{i_R}$ (100mV/div).

Notice that varying R in this way causes the size of the attractors to change: the period-one orbit is large, period-two is smaller, the Rössler-type attractor is smaller again, and the Double Scroll shrinks considerably before it dies.

4 C_1 bifurcation sequence

An alternative way to view the bifurcation sequence is by adjusting C_1. In this case, fix the value of R at 1800 Ω and vary C_1. Monitor v_{C_1} and v_{C_2} as before. The full range of bifurcations from equilibrium through Hopf, period-doubling, Rössler, and Double Scroll can be observed as C_1 is reduced from 12.0 nF to 6.0 nF (see Fig. 9). Unlike the R bifurcation sequence, the size of the Double Scroll attractor remains almost constant here.

5 Limitations

The breakpoints in the nonlinear resistor's $v-i$ characteristic are proportional to the saturation levels of the op amps. The saturation levels in turn are determined by the power supply voltages and by the internal architecture of the op amps. If the levels are different, as they typically are, the resulting $v-i$ characteristic will be asymmetric. This results in a Double Scroll attractor which has one lobe bigger than the other; the effect is illustrated in Fig. 10. Here, we have reduced the negative power supply voltage from 9V to 7V in magnitude. The result is to move the left breakpoint of the $v-i$ characteristic, which in turn produces an asymmetry in the attractor.

While asymmetry may be aesthetically unpleasing, it has little effect on the bifurcation sequence or on the nature of the attractor. If you prefer, the asymmetry may be corrected by adjusting the positive and negative power supply voltages until symmetry is achieved. For example, the negative

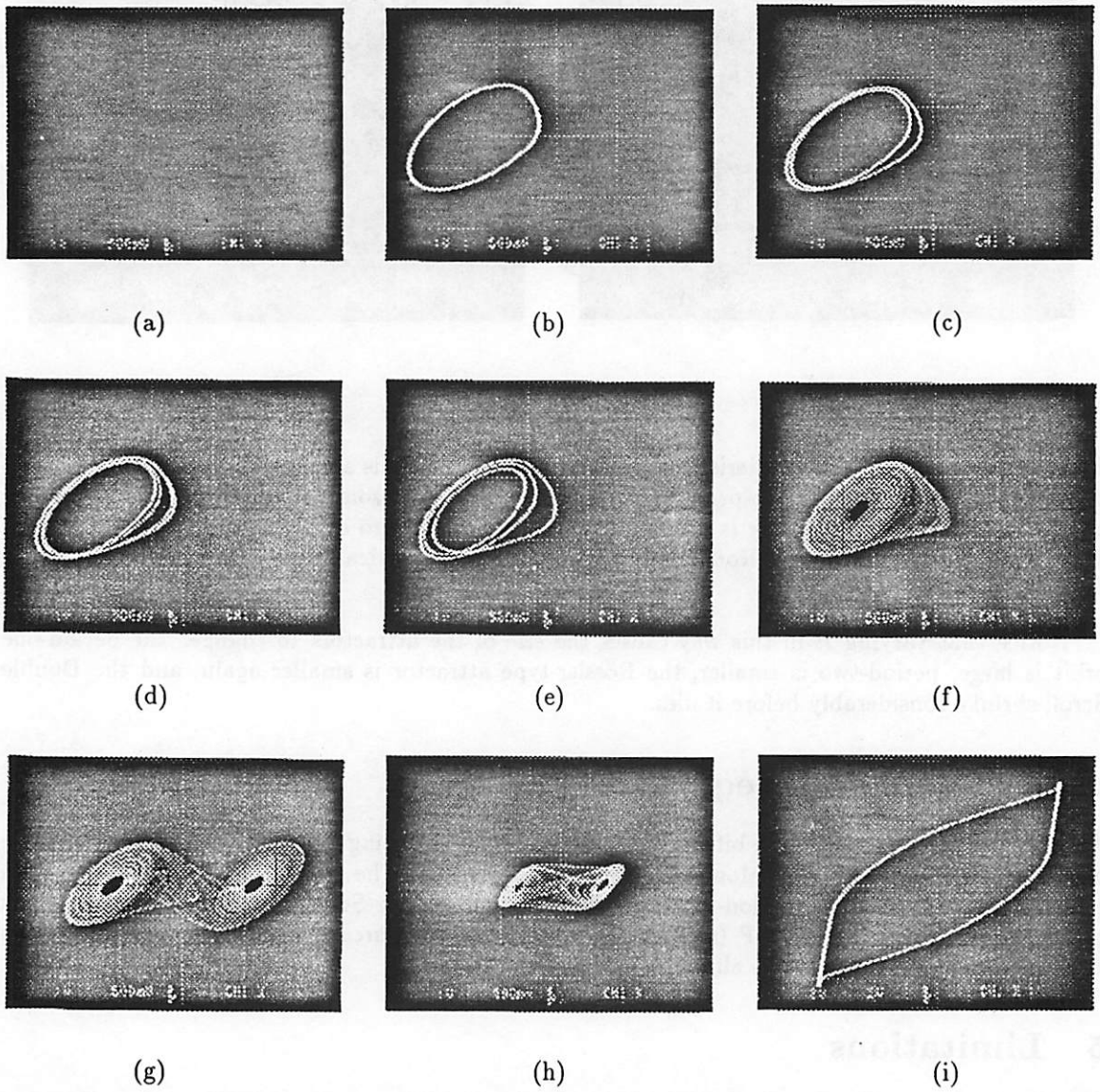

Figure 8: Typical R bifurcation sequence in Chua's circuit (component values as in the table above). Horizontal axis v_{C_1} (a)-(h) 1V/div, (i) 2V/div; vertical axis v_{C_2} (a)-(h) 500mV/div, (i) 2V/div. (a) $R = 2.00k\Omega$, dc equilibrium; (b) $R = 1.88k\Omega$, period-1; (c) $R = 1.85k\Omega$, period-2; (d) $R = 1.84k\Omega$, period-4; (e) $R = 1.825k\Omega$, period-3 window; (f) $R = 1.79k\Omega$, Rössler-type attractor; (g) $R = 1.74k\Omega$, Double Scroll attractor; (h) $R = 1.49k\Omega$, Double Scroll attractor; (i) $R = 1.40k\Omega$, large limit cycle corresponding to outer segments of the $v - i$ characteristic.

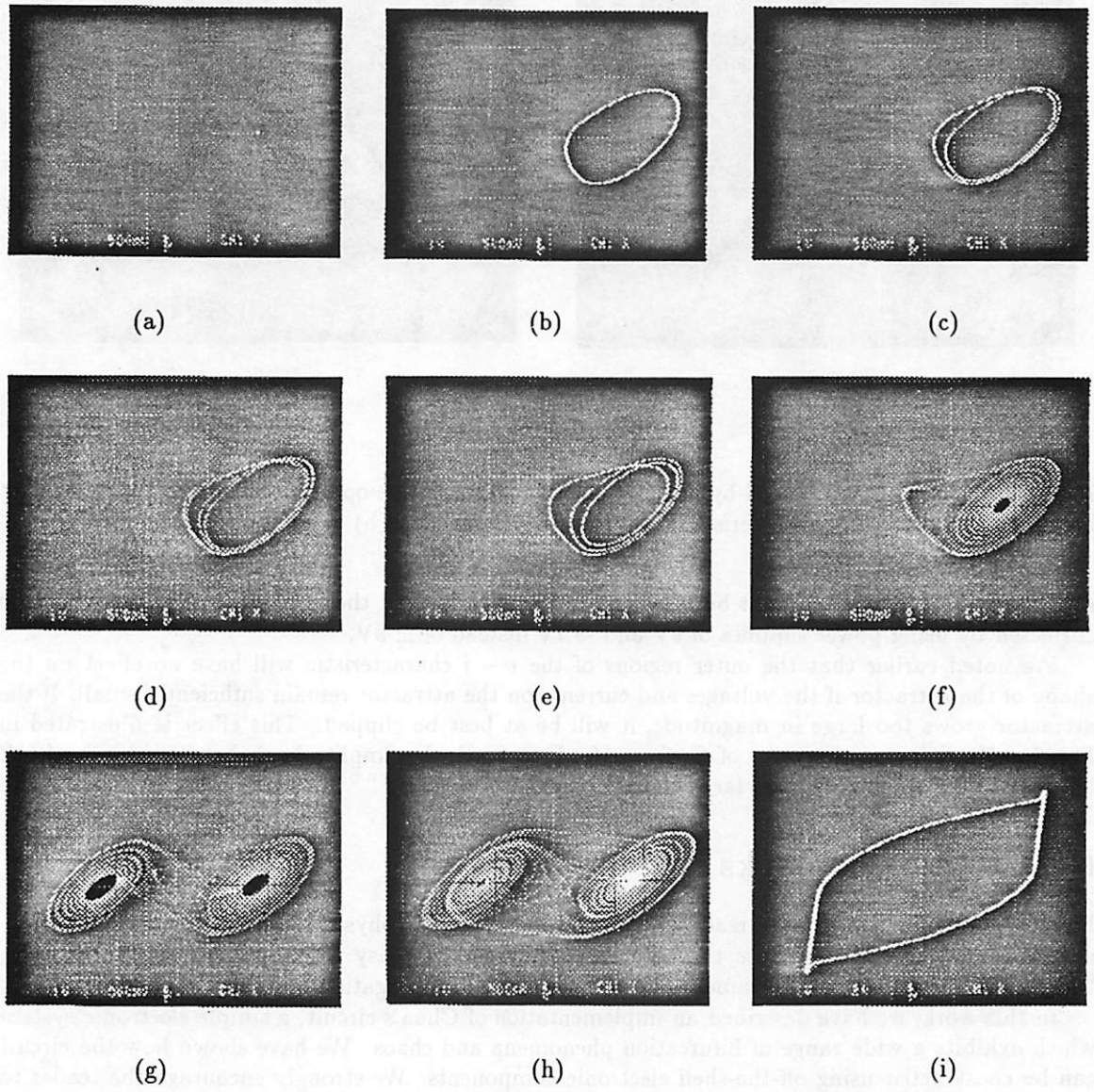

Figure 9: Typical C_1 bifurcation sequence in Chua's circuit (component values as shown in the table above [R = 1800 Ω]). Horizontal axis v_{C_1} (a)-(h) 1V/div, (i) 2V/div; vertical axis v_{C_2} (a)-(h) 500mV/div, (i) 2V/div. (a) $C_1 = 11.0nF$, dc equilibrium; (b) $C_1 = 10.2nF$, period-1; (c) $C_1 = 10.1nF$, period-2; (d) $C_1 = 10.0nF$, period-4; (e) $C_1 = 9.91nF$, period-3 window; (f) $C_1 = 9.7nF$, Rössler-type attractor; (g) $C_1 = 9.4nF$, Double Scroll attractor; (h) $C_1 = 8.0nF$, Double Scroll attractor; (i) $C_1 = 7.0nF$, large limit cycle corresponding to outer segments of the $v - i$ characteristic.

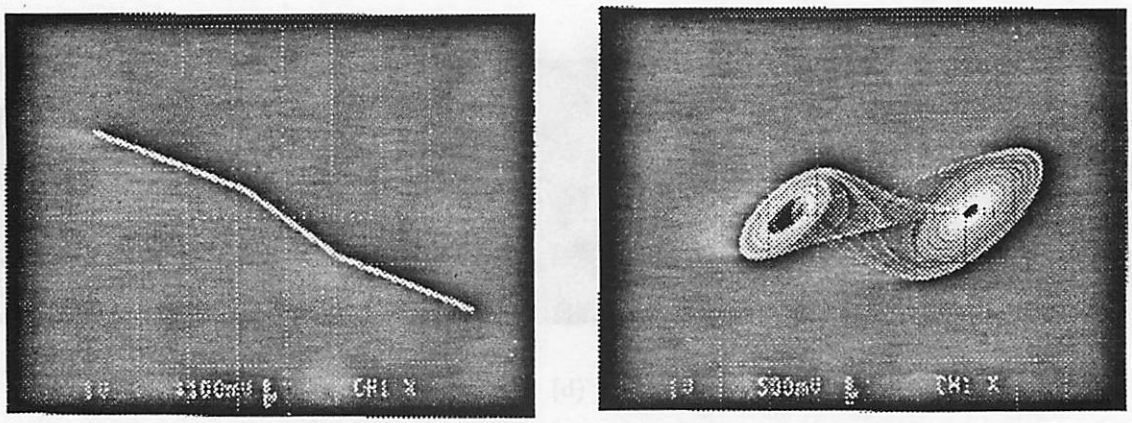

(a) (b)

Figure 10: Asymmetry induced by unequal positive and negative op amp saturation levels. (a) left breakpoint of the $v - i$ characteristic is smaller (in magnitude); (b) attractor is asymmetric.

saturation level typically might be 0.7V less in magnitude than the positive level. This could be corrected by using power supplies of 9V and -9.7V instead of $\pm$ 9V.

We noted earlier that the outer regions of the $v - i$ characteristic will have no effect on the shape of the attractor if the voltages and currents on the attractor remain sufficiently small. If the attractor grows too large in magnitude, it will be at best be clipped. This effect is illustrated in Fig. 11. By reducing the value of C_1 from 10 nF to 8 nF, the amplitude of the attractor in the R bifurcation sequence grows too large and is clipped.

6 Closing Remarks

Electronic circuits are a more readily accessible metaphor for physical systems than mass-spring-damper representations because they are easy to synthesize, easy to build, and easy to analyze. They represent an attractive framework for experimental investigation of dynamical system.

In this work, we have described an implementation of Chua's circuit, a simple electronic system which exhibits a wide range of bifurcation phenomena and chaos. We have shown how the circuit can be constructed using off-the-shelf electronic components. We strongly encourage the reader to build this circuit both for demonstration and research purposes.

7 Acknowledgements

This work was sponsored in part by the National Science Foundation under Grant MIP 89-12639 and by the Office of Naval Research under Grant N00014-89-J-1402. Thanks to F. Shen and K. Slot for their help in preparing earlier drafts of this note. The bibliography of papers on Chua's circuit was prepared by Ms. G. Horn. I am grateful to C.-W. Wu, K. Eckert, and N. Hamilton for verifying the robustness of the circuit presented here by test-building it for me. I am indebted to Bert Shi for making it possible to typeset the photographs.

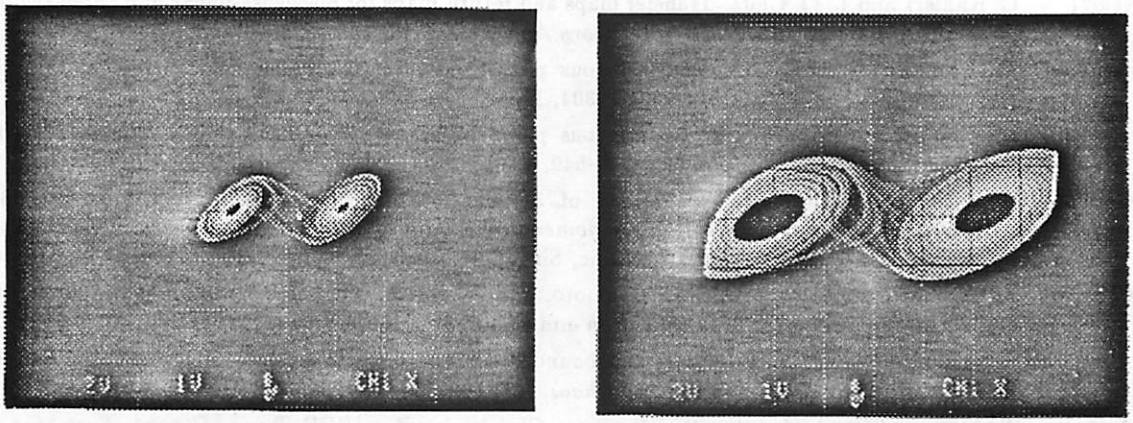

(a) (b)

Figure 11: When the attractor is too large, we cannot neglect the effects of the outer regions of the five-segment $v - i$ characteristic. (a) $C_1 = 10$nF: Double Scroll attractor is restricted to the regions of negative slope; (b) $C_1 = 8$nF: attractor is distorted by the outer positive-going segments.

References

[BC88] P. Bartissol and L. O. Chua. The double hook. *IEEE Trans. Circuits Syst.*, CAS-35(12):1512–1522, 1988.

[Bro87] M. E. Broucke. One-parameter bifurcation diagram for Chua's circuit. *IEEE Trans. Circuits Syst.*, CAS-34(3):208–209, 1987.

[BT90] C. M. Blazquez and E. Tuma. Dynamics of the double scroll circuit. *IEEE Trans. Circuits Syst.*, CAS-37(5):589–593, 1990.

[CC91] J. Cruz and L. O. Chua. First ic implementation of nonlinear resistor in Chua's circuit. (preliminary report), 1991.

[CKM86] L. O. Chua, M. Komuro, and T. Matsumoto. The double scroll family, parts I and II. *IEEE Trans. Circuits Syst.*, CAS-33(11):1073–1118, 1986.

[CL90a] L. O. Chua and G. N. Lin. Canonical realization of Chua's circuit family. *IEEE Trans. Circuits Syst.*, CAS-37(7):885–902, 1990.

[CL90b] L. O. Chua and G. N. Lin. Intermittency in a piecewise-linear circuit. *IEEE Trans. Circuits Syst.*, CAS-38(5):510–520, 1990.

[Kah88a] C. Kahlert. The chaos producing mechanism in Chua's circuit. *Int. J. Circuit Theory Appl.*, 16(4):227–232, 1988.

[Kah88b] C. Kahlert. Dynamics of the inclusions appearing in the return maps of Chua's circuit - 1. the creation mechanism. *Int. J. Circuit Theory Appl.*, 17(1):29–46, 1988.

[Kah88c] C. Kahlert. The range of transfer and return maps in three-region piecewise-linear dynamical systems. *Int. J. Circuit Theory Appl.*, 16:11–23, 1988.

[Kah91] C. Kahlert. Heteroclinic orbits and scaled similar structures in the parameter space of the Chua oscillator. In G. Baier and M. Klein, editors, *Chaotic Hierarchy*, pages 209–234. World Scientific, Singapore, 1991.

[KC87] C. Kahlert and L. O. Chua. Transfer maps and return maps for piecewise-linear and three-region dynamical systems. *Int. J. Circuit Theory Appl.*, 15:23–49, 1987.

[Kom88a] M. Komuro. Normal forms of continuous piecewise-linear vector field and chaotic attractors: Part I. *Japan J. Appl. Math*, 5(2):257–304, 1988.

[Kom88b] M. Komuro. Normal forms of continuous piecewise-linear vector field and chaotic attractors: Part II. *Japan J. Appl. Math*, 5(3):503–549, 1988.

[Kom90] M. Komuro. Bifurcation equations of 3-dimensional piecewise-linear vector fields. In H. Kawakami, editor, *Bifurcation Phenomena in Nonlinear Systems and Theory of Dynamical Systems*, pages 113–123. World Scientific, Singapore, 1990.

[KTMH91] M. Komuro, R. Tokunaga, T. Matsumoto, and A. Hotta. Global bifurcation analysis of the double scroll circuit. *Int. J. Bifurcation and Chaos*, 1(1):139–182, 1991.

[LU91] R. Lozi and S. Ushiki. Confinors and bounded-time patterns in Chua's circuit and the double scroll family. *Int. J. Bifurcation and Chaos*, 1(1):119–138, 1991.

[Mat84] T. Matsumoto. A chaotic attractor from Chua's circuit. *IEEE Trans. Circuits Syst.*, CAS-31(12):1055–1058, 1984.

[MC87] A. I. Mees and P. B. Chapman. Homoclinic and heteroclinic orbits in the double scroll attractor. *IEEE Trans. Circuits Syst.*, CAS-34(9):1115–1120, 1987.

[MCA88] T. Matsumoto, L. O. Chua, and K. Ayaki. Reality of chaos in the double scroll circuit: A computer-assisted proof. *IEEE Trans. Circuits Syst.*, CAS-35(7):909–925, 1988.

[MCK85] T. Matsumoto, L. O. Chua, and M. Komuro. The double scroll. *IEEE Trans. Circuits Syst.*, CAS-32(8):797–818, 1985.

[MCK86] T. Matsumoto, L. O. Chua, and M. Komuro. The double scroll bifurcations. *Int. J. Circuit Theory Appl.*, 14(1):117–146, 1986.

[MCK87] T. Matsumoto, L. O. Chua, and M. Komuro. Birth and death of the double scroll. *Physica*, 24D:97–124, 1987.

[MCT86] T. Matsumoto, L. O. Chua, and K. Tokumasu. Double scroll via a two-transistor circuit. *IEEE Trans. Circuits Syst.*, CAS-33(8):828–835, 1986.

[MCT87] T. Matsumoto, L. O. Chua, and R. Tokunaga. Chaos via torus breakdown. *IEEE Trans. Circuits Syst.*, CAS-34(3):240–253, 1987.

[Ogo87] M. J. Ogorzalik. Chaotic regions from double scroll. *IEEE Trans. Circuits Syst.*, CAS-34(2):201–203, 1987.

[PC87] T. S. Parker and L. O. Chua. The dual double scroll equation. *IEEE Trans. Circuits Syst.*, CAS-34(9):1059–1073, 1987.

[SC88] C. P. Silva and L. O. Chua. The overdamped double scroll family. *Int. J. Circuit Theory Appl.*, 16(7):223–302, 1988.

[TMIM89] R. Tokunaga, T. Matsumoto, T. Ida, and K. Miya. Homoclinic linkage in the double scroll circuit and the cusp-constrained circuit. In N. Aoki, editor, *The Study of Dynamical Systems*, pages 192–209. World Scientific, Singapore, 1989.

[TMK+89] R. Tokunaga, T. Matsumoto, M. Komuro, L. O. Chua, and K. Miya. Homoclinic linkage: A new bifurcation mechanism. *Proc. IEEE ISCAS*, 2:826–829, 1989.

[Wu87] S. Wu. Chua's circuit family. *Proc. IEEE*, 75(8):1022–1032, 1987.

[YL87] L. Yang and Y. L. Liao. Self-similar structures from Chua's circuit. *Int. J. Circuit Theory Appl.*, 15:189–192, 1987.

[ZA85a] G. Q. Zhong and F. Ayrom. Experimental confirmation of chaos from Chua's circuit. *Int. J. Circuit Theory Appl.*, 13(11):93–98, 1985.

[ZA85b] G. Q. Zhong and F. Ayrom. Periodicity and chaos in Chua's circuit. *IEEE Trans. Circuits Syst.*, CAS-32(5):501–503, 1985.